Valorization of CO_2 into *N*-alkyl Oxazolidin-2-ones Promoted by Metal-free Porphyrin/TBACl System: Experimental and Computational Studies

Caterina Damiano[a], Paolo Sonzini[a], Gabriele Manca*[b] and Emma Gallo*[a]

[a] Dr. C. Damiano, Dr. P. Sonzini and Prof. E. Gallo
Department of Chemistry
University of Milan
Via Golgi, 19, I-20133 Milan, Italy
E-mail: emma.gallo@unimi.it; website: https://sites.unimi.it/emmagallogroup/

[b] Dr. G. Manca
Istituto di Chimica dei Composti OrganoMetallici,
ICCOM-CNR
Via Madonna del Piano 10, I-50019 Sesto Fiorentino, Italy
E-mail: gabriele.manca@iccom.cnr.it; www.iccom.cnr.it/index.php/it/istituto/personale2?view=member&task=show&id=132

Supporting information for this article is given via a link at the end of the document.

Abstract: The cycloaddition of CO_2 to *N*-alkyl aziridines were efficiently promoted by the convenient $TPPH_2$/TBACl binary catalytic system. The metal-free procedure was effective for the synthesis of differently substituted *N*-alkyl oxazolidin-2-ones in yields up to 100% and excellent regioselectivities (up to 99%). The mechanism of the reaction was proposed on the basis of a DFT study which indicated the formation of an adduct between $TPPH_2$ and TBACl as the effective catalytic active species.

Introduction

The progressive increasing of greenhouse gas emissions is causing a constant rising in average global temperatures which is responsible for extreme events all over the world. In order to reverse this no longer sustainable trend, it is imperative to reduce damaging emissions and develop sustainable circular chemical processes, in which gaseous wastes are valorized as new resources for the synthesis of fine-chemicals.

Since carbon dioxide is one of the most harmful emissions for the environment, the use of CO_2 as a renewable, cheap and nontoxic C1 synthetic building block is receiving increasing scientific attention.[1] Among all synthetic routes employing CO_2 as a starting material, ring-insertion processes in epoxides and aziridines represent 100% atom-efficient procedures for the eco-compatible production of cyclic carbonates[2] and oxazolidinones,[3] respectively.

Oxazolidinones constitute a versatile class of compounds which, depending on substituents present on the molecular skeleton, can be employed as synthetic intermediates,[4] chiral auxiliaries in organic synthesis[5] and pharmaceuticals.[6] In particular, the oxazolidinone motif is found in antimicrobial drugs,[7] such as Linezolid[8] and Tedizolid,[9] antidepressants, such as Toloxatone[10] and also in anti-cancer medicaments.[11]

The catalyzed CO_2 cycloaddition to aziridines usually occurs in the presence of an electrophile/nucleophile (E/Nu) binary system, where the electrophile is in charge of coordinating the nitrogen aziridine atom in order to promote the opening of the aziridine ring by the nucleophilic species (Scheme 1).

As reported in Scheme 1, the reaction produces two regioisomers A and B (5- and 4-substituted oxazolidin-2-one, respectively) in accordance with the presence of two inequivalent aziridine carbon atoms where the nucleophilic attack can take place.

It should be noted that while the electrophile is usually considered the reaction catalyst, the nucleophilic species, such as quaternary ammonium salts or other Lewis bases (LB), is indicated as the co-catalyst of the CO_2 cycloaddition.

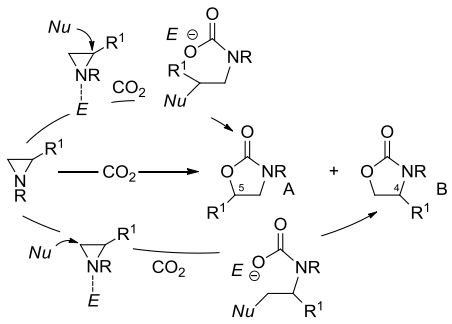

Scheme 1. General scheme of the CO_2 cycloaddition to aziridine mediated by the E/Nu binary system.

Even if the insertion of CO_2 into aziridines can proceed in the presence of the sole co-catalyst[12] and neither the solvent[13] nor catalyst[1b, 14] are necessary, a great improvement of the reaction productivity (higher yields and regioselectivities) and experimental conditions sustainability (lower CO_2 pressures, lower temperatures and reduced reaction times) is generally observed when the reaction is mediated by either homogeneous[15] or heterogeneous[3a, 16] catalysts.

Among all catalytic systems, which promote the CO_2 cycloaddition to three-membered rings (epoxides and aziridines), those employing porphyrin metal catalysts in the presence of LB co-catalysts[15b, 17] performed well under low CO_2 pressures and temperatures.

In the last few years we have studied the performance of porphyrin-based protocols in catalyzing the CO_2 cycloaddition to both epoxides and aziridines. Besides the capacity of ruthenium porphyrins in mediating both reactions,[18] we have more recently discovered that the CO_2 cycloaddition to *N*-aryl aziridines performed well in the presence of metal-free porphyrin catalysts.[19] The $TPPH_2$/TBACl ($TPPH_2$ = *meso*-tetrakis phenyl porphyrin; TBACl = tetrabutyl ammonium chloride) system demonstrated to be a convenient combination for synthesizing *N*-aryl oxazolidin-2-ones. The study of the reaction scope, using the optimized experimental conditions of 125 °C, 1.2 CO_2 MPa and $TPPH_2$/TBACl/aziridine = 1:5:100, revealed a large applicability of the protocol and a good tolerance of different functional groups. In addition, the DFT investigation of the reaction mechanism clarified the nature of species involved in the catalytic cycle.

Results and Discussion

Synthetic Study

In view of the aforementioned results and the importance of developing metal-free sustainable catalytic procedures, we here present the synthesis of *N*-alkyl oxazolidin-2-ones by applying the protocol described above for obtaining *N*-aryl derivatives.[19]

Table 1. Synthesis of oxazolidin-2-ones **1** and **2** mediated by porphyrin/TBACl catalytic system.

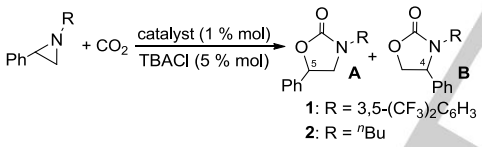

entry	catalyst	yield **1** (%)[b] A/B ratio[b]	yield **2** (%)[b] A/B ratio[b]
1	$TPPH_2$	95 87:13	95[c] 95:5
2	4-^{t}BuTPPH_2	69 83:17	94[c] 91:9
3	4-CF_3TPPH_2	61 85:15	80[c] 92:8
4	4-COOHTPPH_2	84 86:14	99[c] 86:14
5	F_5TPPH_2	69 87:13	76[c] 88:12
6	F_{20}TPPH_2	43 84:16	74[c] 89:11
7	OEPH_2	63 84:16	85[c] 93:7

[a] Reaction conditions: 1.5 M aziridine THF solution in a steel autoclave for 3 hours with catalyst/TBACl/aziridine = 1:5:100 at 125°C and 1.2 MPa of CO_2. [b] Determined by ^{1}H NMR using 2,4-dinitrotoluene as the internal standard. [c] After 1 hour.

In order to compare the reactivity of *N*-aryl aziridines with that of *N*-alkyl aziridines, two model reactions producing oxazolidin-2-ones **1** and **2** were performed in the presence of the co-catalyst TBACl and different free porphyrins for also assessing the dependence of the reaction productivity from the chemical characteristics of the catalyst. The catalytic efficiency of the different porphyrins employed was tested by running the synthesis of **1** and **2** for only 3 hours and 1 hour respectively, in order to avoid the complete aziridine conversion (Table 1).

Results of Table 1 show a general more pronounced reactivity of *N*-alkyl aziridines with respect to *N*-aryl aziridines and in fact, better yields and A/B ratios were always registered. Catalytic data did not suggest a real dependence of the reaction performance on the electronic characteristic of the substituent placed in the *para* position of the porphyrin *meso* aromatic rings.

In fact, only a slight improvement of yields was achieved by synthesizing **1** and **2** oxazolidin-2-ones in the presence of *meso*-tetrakis(4-tert-butylphenyl) porphyrin (4-^{t}BuTPPH_2) (entry 2, Table 1) rather than *meso*-tetrakis(4-trifluoromethylphenyl) porphyrin (4-CF_3TPPH_2) (entry 3, Table 1) catalyst. The poor electronic effect of the *para*-substituent on the catalytic performance was also suggested on the basis of the similar regioselectivities always achieved independently from the catalyst employed. Among all the porphyrins tested, the best yield of **1** and **2** was obtained by applying $TPPH_2$ and *meso*-tetrakis(4-carboxyphenyl) porphyrin (4-COOHTPPH_2) (entries 1 and 4, Table 1) respectively, while the best regioselectivity was registered by performing the reaction in the presence of $TPPH_2$ (entry 1, Table 1)

On the other hand, the steric behavior of the catalyst influenced the catalytic activity more, as suggested by the lower performances observed by using 5-(pentafluorophenyl)-10,15,20-triphenyl porphyrin (F_5TPPH_2) (entry 5, Table 1). As expected, the negative effect increased by replacing F_5TPPH_2 with *meso*-tetrakis(pentafluorophenyl) porphyrin ($F_{20}TPPH_2$) (entry 6, Table 1), which shows on the catalyst skeleton four pentafluorophenyl moieties instead of only one. The effect was more marked in the synthesis of **1** due to the presence of the more sterically encumbered aromatic group on the aziridine nitrogen atom. It should be noted that the use of octaethylporphyrin ($OEPH_2$), showing ethyl substituents on porphyrin pyrrolic groups, was responsible for a minor negative outcome on the reaction productivity (entry 7, Table 1). However, the analysis of collected data revealed a limited influence of the electronic and steric characteristics of the employed porphyrin on catalytic performances.

It is worth mentioning that the presence of porphyrin had a general positive effect on catalytic reactions, which, if conducted by using TBACl alone under experimental conditions reported in Table 1, produced **1** and **2** in 54% (A/B = 85:15) and 80% (A/B = 90:10) yields, respectively.

Thus, in consideration of the good catalytic results (entry 1, Table 1) observed by employing unsubstituted $TPPH_2$ and due to its commercial availability at a reasonable cost, $TPPH_2$ was used to test the activity of the other tetrabutyl ammonium salts TBAB and TBAI. By using the same experimental conditions reported in Table 1, **2**A/**2**B were formed after one hour of reaction with yield of 27% (A/B = 97:3) and 42% (A/B = 98:2) in the presence of TBAB and TBAI, respectively.

In view of collected results, the $TPPH_2$/TBACl binary system was chosen for studying the reaction scope of the *N*-alkyl oxazolidinone synthesis.

Compounds reported in Table 2 were obtained by running the reaction at 125°C and 1.2 CO_2 MPa in the presence of 1% mol of $TPPH_2$ and 5% mol of TBACl. The reaction time was increased from 1 hour (Table 1) to 6 hours to maximize the productivity and in fact, **2**A/**2**B compounds were formed in a 100% yield (instead than 95%). However, an identical **2**A/**2**B ratio was observed in the two cases (compare Tables 1 and 2), suggesting the independence of the regioselectivity on the reaction time.

Table 2. Synthesis of *N*-alkyl oxazolidin-2-ones **2**-**9** mediated by $TPPH_2$/TBACl catalytic system

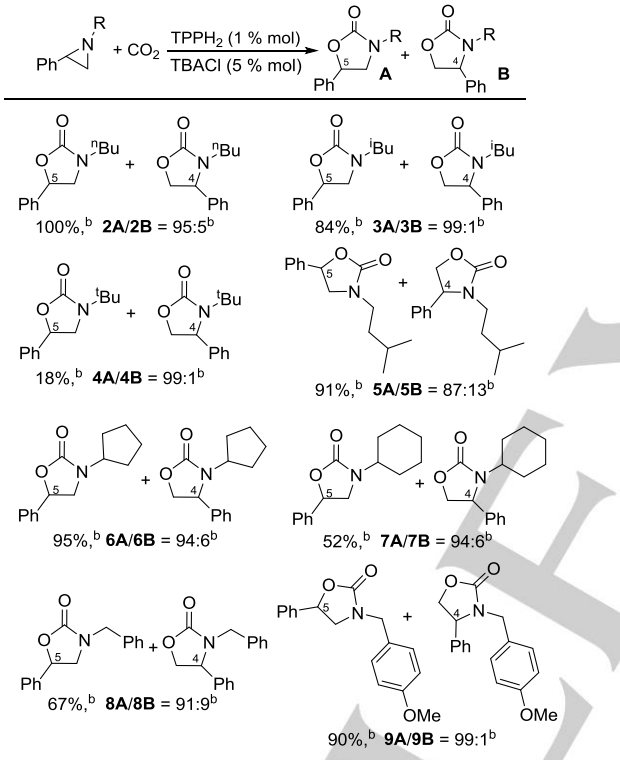

[a] Reaction conditions: 1.5 M aziridine THF solution in a steel autoclave for 6 hours with $TPPH_2$/TBACl/aziridine = 1:5:100 at 125°C and 1.2 MPa of CO_2. [b] Determined by ^1H NMR using 2,4-dinitrotoluene as the internal standard.

The study of the reaction scope disclosed again that one of the most important parameters influencing the catalytic performance is the steric hindrance on the aziridine nitrogen atom.

As showed in Table 2, a decrease of the reaction yield was observed by replacing the ^{n}Bu group on the nitrogen (**2**A/**2**B 100% yield) with ^{i}Bu substituent (**3**A/**3**B 84% yield). Then, when the more encumbered ^{t}Bu group was present on the aziridine nitrogen center, the reaction yield drastically dropped to 18% (**4**A/**4**B). This observation was also supported by the good yield achieved in the synthesis of **5**A/**5**B where, the linearity of the chain, linked to the nitrogen, should allow the approach of the aziridine to the catalytic active center and in turn its conversion into corresponding oxazolidinones **5**A/**5**B. The same trend was observed in the synthesis of compounds **6**A/**6**B and **7**A/**7**B. The enlargement of the ring linked to *N*-aziridine atom caused the evident reduction of the reaction yield from 95% to 52%. Also in this case, the steric hindrance of the starting aziridine did not affect the regioselectivity and the A/B ratio was 94:6 in both cases.

The reaction of *N*-benzylic aziridines occurred in good yields probably for the presence of the CH_2 spacer, which allowed the access of the incoming reagent to the catalytic center. Compounds **8**A/**8**B and **9**A/**9**B were obtained in 67% and 90% yields, respectively.

It is important to underline that all the yields reported in Tables 1 and 2 correspond to the substrate conversion because for all tested aziridines a 100% of reaction selectivity was registered.

In order to explore the asymmetric version of the methodology, the synthesis of **2**A/**2**B was performed in the presence of the chiral porphyrin P* (Figure 1), which already demonstrated to be a good chiral ligand to promote iron-based olefin cyclopropanations.[20]

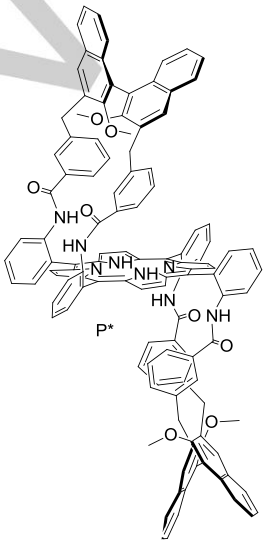

Figure 1. Structure of chiral porphyrin P*

Due to the general difficulty to accomplish stereoselective ring-opening processes, the reaction formed a racemic mixture of **2**A (99% yield, **2**A/**2**B = 90:10) in the presence of P*/TBACl/aziridine = 1:10:100 at 50°C and 1.2 MPa of CO_2. Thus, future efforts will be devoted to investigate the stereospecific transformation of enantiopure aziridines into corresponding chiral oxazolidinones by fine-tuning the reported protocol.

Considering the very good results achieved by employing bifunctional porphyrin catalysts in the CO_2 cycloaddition to epoxide,[21] we modified $F_{20}TPPH_2$ by replacing one pentafluoro *meso*-aryl group with an aromatic moiety, displaying the ammonium salt $N(Bu)_3Cl$ at the end of a carbon chain. It should be noted that the presence of three CH_2 groups between the tetrapyrrolic core and the co-catalyst should allow good arm mobility for shaping the molecular skeleton to the incoming reagent.

The poor catalytic activity of the $F_{20}TPPH_2$/TBACl system (entry 6, Table 1), observed in the synthesis of **2**A/**2**B, should permit a better evaluation of any positive effect deriving from the employment of a bifunctional catalyst in place of a binary

porphyrin/ammonium salt combination. The reaction of porphyrin **10**[22] with $N(Bu)_3$ in the presence of KCl yielded **11** (Scheme 2), which mediated the synthesis of **2**A/**2**B in 49% yield and 99:1 A/B ratio.

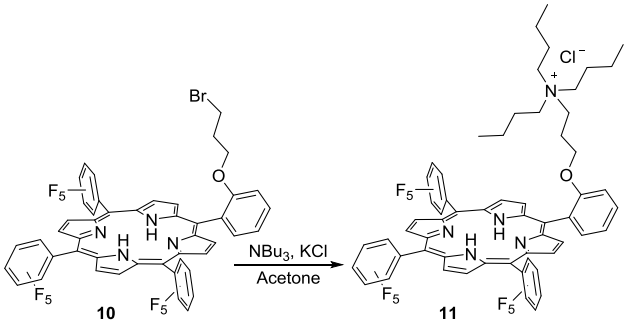

Scheme 2. Synthesis of porphyrin **11**.

As **2**A/**2**B were obtained with 74% yield and A/B ratio of 89:11 in the presence of $F_{20}TPPH_2$/TBACl system (entry 6, Table 1), the use of the bifunctional catalyst **11** had only a positive effect on the reaction regioselectivity with a contemporary decrease of the reaction yield. The unsatisfactory result in term on the reaction productivity can be due either to the requirement of a molar excess of the ammonium salt during the catalysis (porphyrin/TBACl are usually employed in the 1:5 ratio) or the limited mobility of the $N(Bu)_3Cl$ group during the catalytic process.

In order to shed some light on the reaction mechanism and clarify the role of the free porphyrin in mediating the CO_2 cycloaddition to aziridine, a DFT study was undertaken and results are illustrated in the next paragraph.

Theoretical Investigation

The theoretical study of the of *N*-aryl oxazolidin-2-one synthesis, recently reported by us,[19] suggested the catalytic cycle shown in Scheme 3. The adduct **12**, originated by the interaction of $TPPH_2$ with TBACl, reacted with *N*-aryl aziridine (aryl = $3,5(CF_3)_2C_6H_3$) forming **13**, which evolves to **14** by a ring opening reaction due to the nucleophilic attack of Cl^- to the aziridine carbon atom. Thus, the so-obtained electron-rich nitrogen atom activates CO_2 yielding **15**, whose negatively charged oxygen atom provokes the displacement of the chloride atom and the final **1**A formation as the major regioisomer. The overall free energy gain for the reaction was estimated to be exergonic by -2.2 kcal mol^{-1}.

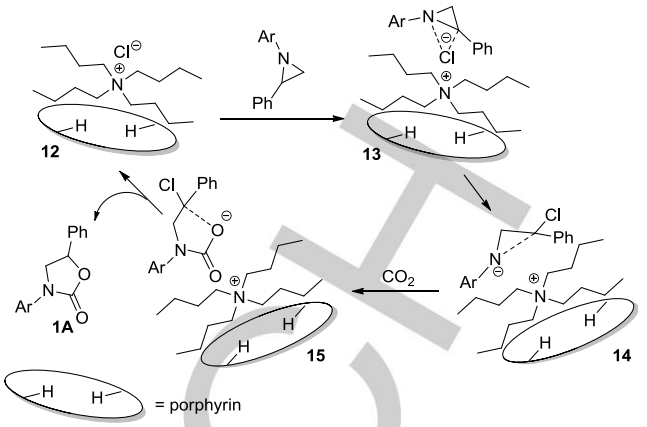

Scheme 3. Proposed mechanism of the *N*-aryl oxazolidin-2-one **1**A formation.

In order to study the similarities and differences between the CO_2 cycloaddition to *N*-aryl and *N*-alkyl aziridines, the latter was theoretically analyzed by considering the effect of the substituents onto the porphyrin macrocycle in the formation and stabilization of the porphyrin/TBACl adduct. In addition, the lack of advantages of using the bifunctional catalyst **11** was also investigated.

In order to rationalize data, which were obtained by using either the most catalytically active 4-$COOHTPPH_2$ (entry 4, Table 1) or the encumbered and less performing $F_{20}TPPH_2$ porphyrin (entry 6, Table 1), the reaction of these two porphyrins with TBACl, producing corresponding adducts **16** and **17**, was modelled by DFT and compared to the formation of adduct **12** (Scheme 3).

Computational analysis revealed no significant difference in the assembly of the two adducts **16** and **17**, which occurred with energy variations -5.8 and -4.5 kcal mol^{-1}, respectively. It is worth noting that the formation of both adducts was less convenient than the synthesis of **12**, which took place with an energy gain of -7.5 kcal mol^{-1}. However, in all the three cases the generation of the catalyst/co-catalyst adduct is a favorite process that explains the positive role of both promoters in favoring the CO_2 cycloaddition.

Considering the negligible energy difference related to the establishment of the two adducts **16** and **17** and the use of $TPPH_2$ for studying the reaction scope (Table 2), all the subsequent calculations were carried out by using adduct **12** as the first step of the **2**A (Table 2) formation.

The reaction of **12** with *N*-butyl aziridine yielded adduct **18** (Figure 2) with a free energy cost of +4.9 kcal mol^{-1}.

Relaxed scan, obtained by a stepwise shortening of the Cl---C_1 distance, revealed the presence of the Transition State $\mathbf{18_{TS}}$ (Figure 2) which was optimized and achieved with a free energy barrier of 35.4 kcal mol^{-1}. The high value of energy, needed for reaching the TS, can explain the high temperature required for the accomplishment of the CO_2 cycloaddition (see experimental).

From a structural viewpoint, $\mathbf{18_{TS}}$ presents a Cl---C_1 distance of 2.12 Å and an elongation of N_2---C_1 distance up to 2.22 Å. The Transition State nature of $\mathbf{18_{TS}}$ was confirmed by the detection of a single imaginary frequency at -230.1 cm^{-1} associated with the shortening of the Cl---C_1 distance and simultaneous elongation of the N_2---C_1 bond.

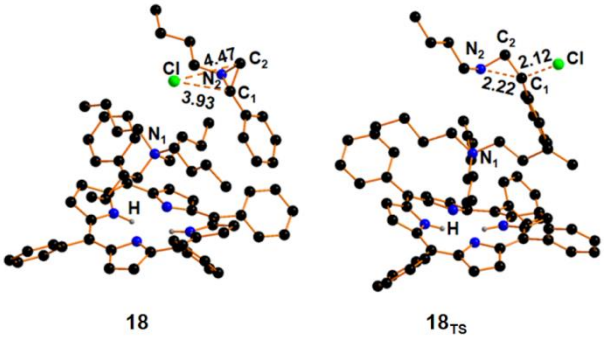

Figure 2. Optimized structures of **18** and **18$_{TS}$**. Hydrogen atoms are omitted for clarity.

After the Transition State, compound **19**, showing a lengthening of the N_2---C_1 distance to 2.33 Å and a shortening of C_1---Cl bond to 1.91 Å, was obtained (Figure 3). The modest free energy gain of -2.2 kcal mol^{-1} revealed a limited stabilization of the negative charge at the N_2 atom which is responsible for an efficient interaction of **19** with CO_2.

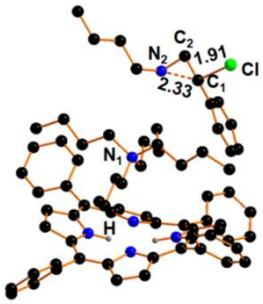

Figure 3. Optimized structure of **19**. Hydrogen atoms are omitted for clarity.

In fact, the synthesis of species **20** (Figure 4), was favored by **-**20.3 kcal mol^{-1}, as also certified by the modelled IR C=O stretching at *ca*. 1575 cm^{-1}. Compound **20** displayed a bent CO_2 moiety with the $O_1C_3O_2$ angle of 127° and the strong N_1---C_3 bond of 1.44 Å. The final synthesis of the major regioisomer *N*-butyl oxazolidin-2-one **2**A occurred through the formation of the Transition State **20$_{TS}$** (Figure 4) with a free energy barrier of +9.4 kcal mol^{-1}. The modelling of compound **20$_{TS}$** revealed a *quasi*-linearity of the O_1C_1Cl angle (177°) and a trigonal bipyramidal molecular geometry around the C_1 atom (Figure 4, the hydrogen atom was omitted for clarity), which coordinated the approaching O_1 nucleophile and the leaving Cl anion as axial ligands. The Transition State nature of **20$_{TS}$** was confirmed by the detection of a single imaginary frequency at -188.1 cm^{-1}, which was associated with the approaching of O_1 to C_1 and the consequent departure of Cl.

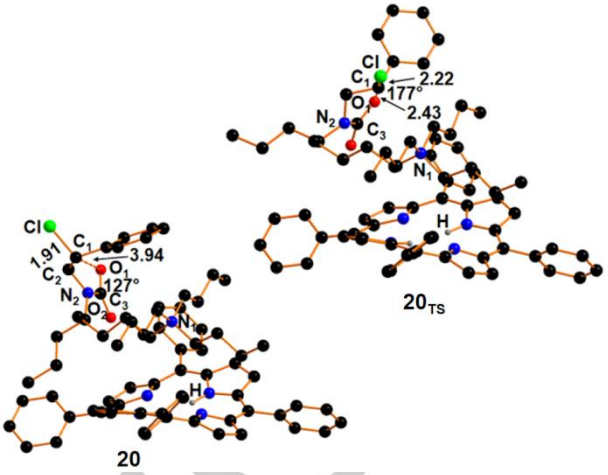

Figure 4. Optimized structures of **20** and **20$_{TS}$**. Hydrogen atoms were omitted for clarity.

After the accomplishment of the Transition State **20$_{TS}$**, the final product **2**A was achieved with an energy gain of -31.9 kcal mol^{-1}. In conclusion, the entire free energetic profile of the CO_2 cycloaddition to *N*-butyl aziridine yielding **2**A occurred with an overall free energy gain of -4.7 kcal mol^{-1}, as shown in Figure 5. This value was larger than the overall free energy gain of -2.2 kcal mol^{-1} which was calculated for the CO_2 cycloaddition to *N*-aryl aziridines. The energetic difference between the two processes is in accordance to the general higher reactivity of the *N*-alkyl with respect to *N*-aryl aziridines towards CO_2 in the presence of free porphyrin molecules (Table 1).

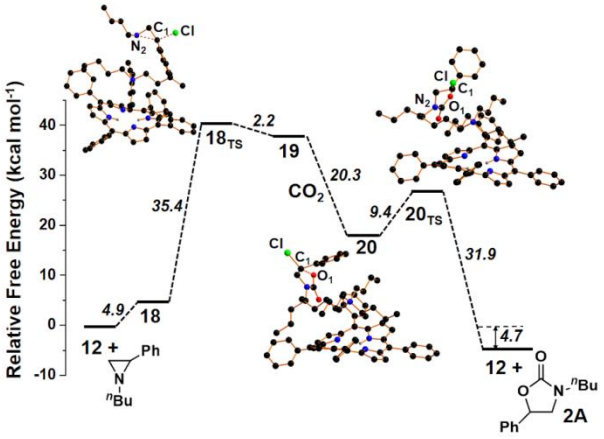

Figure 5. Free energy profile of synthesis of **2**A.

As discussed in the precedent paragraph, the bifunctional porphyrin **11** was synthesized and tested to assess a possible positive catalytic improvement of placing both the catalyst and co-catalyst onto the same molecular skeleton. Unfortunately, experimental results did not suggest any advantage of using **11** instead of the binary porphyrin/TBACl combination.

Thus, to better understand the lack of any beneficial effect when the bifunctional catalyst was employed to promote the synthesis of **2**A, the structure of **11** was first modelled by DFT calculations and compared to the X-ray molecular structure of a similar

porphyrin,[22] presenting a $N(Et)_3I$ group instead of the $N(Bu)_3Cl$ moiety of **11**. The DFT investigation was conducted in THF solution and confirmed that, analogously to what observed in the solid state, the ammonium cation lies on the tetrapyrrolic core probably thanks to dispersion forces between the macrocycle and the alkyl chains (Figure 6). The interaction of **11** with the incoming *N*-butyl aziridine yielded adduct **21** (Figure 6) with a high free energy cost of +9.7 kcal mol^{-1}. The disfavoring energy contribution was also confirmed by the large separation between the chloride anion and the C_1 center, which is 1.4 Å ca. longer than in adduct **18** and implies a less favorite attack of the chloride nucleophile to the aziridine carbon atom.

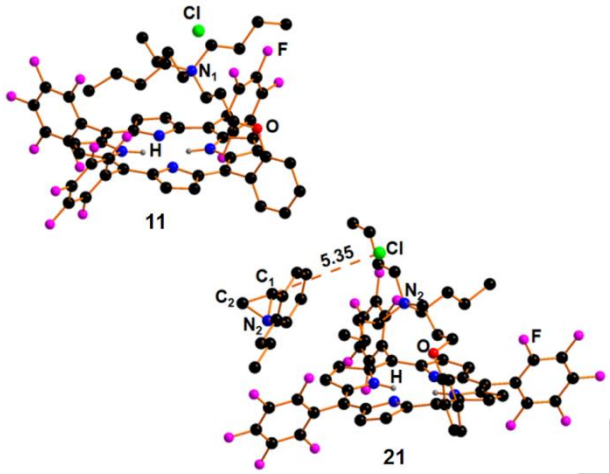

Figure 6. Optimized structure of **11** and **21**.

In view of the obtained computational and experimental results, the formation of *N*-butyl oxazolidin-2-one **2**A promoted by the bifunctional porphyrin **11** was not investigated further.

Conclusion

The present manuscript reported the catalytic activity of the $TPPH_2$/TBACl combination for the synthesis of *N*-alkyl oxazolidin-2-ones. Among all catalytic reactions involving either harmful metal catalysts or promoters, which are often obtained through time-consuming procedures, the present protocol consists of an eco-compatible, commercially available and low-cost methodology. In addition, the low catalytic loading as well as the moderate CO_2 pressure and temperature required further favor the general application of the catalytic procedure in every laboratory. The study of the role of the porphyrin skeleton in modulating the catalytic efficiency revealed only a slight dependence of the activity on the steric hindrance of the macrocycle. The electronic behavior of the catalyst seems to not affect the reaction performance.

The mechanism was proposed on the basis of DFT calculations which revealed that the reaction between the porphyrin and TBACl yielded an adduct, which was exoergonically formed and can be considered the real catalytic active species of the reaction.

Finally, the bifunctional catalyst **11**, showing the ammonium salt co-catalyst on the porphyrin skeleton, was synthesized but was less efficient than the binary porphyrin/ammonium salt combination.

Since the $TPPH_2$/TBACl adduct is able to activate aziridine ring towards a nucleophilic attack, the present report can open the door to its use in other reactions where the ring-opening process of aziridine is the key-step of the catalytic cycle.

Experimental Section

General methods. Unless otherwise specified, all the reactions were carried out under nitrogen atmosphere by employing standard Schlenk techniques and magnetic stirring. THF and benzene were distilled over sodium and benzophenone and kept under nitrogen. Styrene was distilled over calcium hydride and kept under nitrogen. Acetone was distilled over calcium sulfate and kept under nitrogen. *meso*-Tetrakis phenyl porphyrin ($TPPH_2$),[23] 5-(pentafluorophenyl)-10,15,20-triphenyl porphyrin (F_5TPPH_2),[24] *meso*-tetrakis(pentafluorophenyl) porphyrin ($F_{20}TPPH_2$),[25] octaethylporphyrin ($OEPH_2$),[26] *meso*-tetrakis(4-trifluoromethylphenyl) porphyrin ($4\text{-}CF_3TPPH_2$),[27] *meso*-tetrakis(4-tert-butylphenyl) porphyrin ($4\text{-}^tBuTPPH_2$),[28] *meso*-tetrakis(4-carboxyphenyl) porphyrin ($4\text{-}COOHTPPH_2$)[29] and 5-(2-(3-bromopropoxy)phenyl)-10,15,20-trispentafluorophenylporphyrin (**10**)[22] were all synthesized following reported procedures. 1-(3,5-*bis*-Trifluoromethylphenyl)-2-phenylaziridine[30] and all the *N*-alkyl aziridines were synthesized following reported procedure.[18a] All the other starting materials were commercial products and used as received. NMR spectra were recorded at room temperature either on a Bruker Avance 300-DRX, operating at 300 MHz for ^1H, at 75 MHz for ^{13}C and at 282 MHz for ^{19}F or on a Bruker Avance 400-DRX spectrometers, operating at 400 MHz for ^1H and at 100 MHz for ^{13}C and at 376 MHz for ^{19}F. Chemical shifts (ppm) are reported relative to TMS. The ^1H NMR signals of the compounds described in the following were attributed by 2D NMR techniques. Assignments of the resonances in ^{13}C NMR were made by using the APT pulse sequence, HSQC and HMBC techniques. Infrared spectra were recorded on a Varian Scimitar FTS 1000 spectrophotometer. UV/Vis spectra were recorded on an Agilent 8453E instrument. Elemental analyses and mass spectra were recorded in the analytical laboratories of Milan University.

Synthesis of 5-(2-(3-(butyl)$_3$ammoniumpropoxy)phenyl)-10,15,20-trispentafluorophenylporphyrin chloride (11). 5-(2-(3-Bromopropoxy)phenyl)-10,15,20-trispentafluorophenylporphyrin (**10**) (100 mg, 0.133 mmol), tributylamine (246 mg, 1.33 mmol) and KCl (99 mg, 1.33 mmol) were dissolved in 10 mL of dry acetone and refluxed for 72 hours. Then, the solvent was evaporated to dryness and the reddish residue was purified by flash chromatography (SiO_2, gradient elution from DCM to DCM/MeOH 97:3) to get the purple solid **11** (25% yield). ^1H-NMR (400 MHz, $CDCl_3$): δ 9.01 – 9.00 (m, 2H, $H^{\beta pyrr}$), 8.93 – 8.92 (m, 6H, $H^{\beta pyrr}$), 8.05 – 8.03 (m, 1H, H^{Ar}), 7.88 – 7.83 (m, 1H, H^{Ar}), 7.56 – 7.41 (m, 2H, H^{Ar}), 1.58 – 1.53 (m, 2H, H^{CH2}) 1.47 – 1.38 (m, 10H, H^{CH2}) -0.23 (t, *J* = 6.9 Hz, 9H, H^{CH3}), -0.33 – -0.47(m, 12H, H^{CH2}), -2.88 ppm (s, 2H, H^{NH}). ^{19}F NMR (376 MHz, $CDCl_3$) δ -136.39 (m, 3F), -137.54 (dd, *J* = 24.6, 8.5 Hz, 1F), -137.79 (m, 2F), -150.71 (t, *J* = 20.9 Hz, 2F), -151.00 (t, *J* = 20.9 Hz, 1F), -160.62 (td, *J* = 22.4, 8.4 Hz, 2F), -160.77 – -161.08 (m, 3F), -161.29 ppm (td, *J* = 22.4, 8.4 Hz, 1F). ^{13}C NMR (101 MHz, $CDCl_3$) δ 157.67, 147.82, 145.35, 143.65, 141.09, 138.91, 136.45, 134.87, 131.32, 129.76, 121.05, 119.52, 115.48, 113.47, 102.98, 102.32, 77.34, 64.80, 57.08, 54.39, 22.36, 21.85, 17.85, 12.26 ppm. LR-MS (ESI): m/z calcd for ($C_{59}H_{47}ClF_{15}N_5O$): 1162.49, found 1126.6 [M^+], 35.4 [X^-]. Elemental Analysis calcd. for ($C_{59}H_{47}ClF_{15}N_5O$): C (60.96), H (4.08), N (6.02), found: C (61.78), H (4.95), N (6.65). UV-Vis λ_{max} (DCM)/nm (log ε): 414 (5.18), 508 (4.00), 539 (3.17) 584 (3.52) 637 (2.89). IR ν_{max} (DCM)/cm^{-1}: 3322, 3058, 2986, 2961, 2931, 2874, 2860, 1650, 1519, 1499, 1482, 1266, 990. Pf > 350°C.

General catalytic procedure. In a 2.0 mL glass liner equipped with a screw cap and glass wool, the desired catalyst (3.75 x 10^{-6} mmol), TBACl (5.2 mg, 1.87 x 10^{-5}mmol) and aziridine (3.75 x 10^{-4} mmol) were dissolved in dry THF (0.250 mL). The reaction mixture was cooled to -78°C and the vessel was transferred into a stainless-steel autoclave; three vacuum-nitrogen cycles were performed and 1.2 MPa of CO_2 was charged at room temperature. The autoclave was placed in a preheated oil bath at 125°C and stirred for the required time (see Tables 1 and 2), then it was cooled at room temperature and slowly vented. The solvent was evaporated to dryness and the crude analyzed by ^{1}H NMR spectroscopy by using 2,4-dinitrotoluene as the internal standard.

Computational Details. All the minima and Transition States along the reaction pathway were isolated and characterized at B97D-DFT level of theory.[31][32] All the optimized structures were validated as minima or Transition States by the vibrational frequencies calculations. All the calculations were carried out within the CPCM model[33] for the tetrahydrofuran, the solvent that was experimentally used. The 6-31G basis set, with the addition of the polarization functions (d, p) was adopted. The coordinates of all the optimized structures are reported in the Supporting Information.

Acknowledgements

CD, PS and EG gratefully acknowledge the University of Milan-Italy for PSR 2020 – financed project ‘‘Sustainable catalytic strategies for the synthesis of high added-value fine-chemicals”

Keywords: oxazolidinone • carbon dioxide • porphyrin • aziridine • catalysis

[1] a) A. W. Kleij, M. North, A. Urakawa, *ChemSusChem* **2017**, *10*, 1036-1038; b) C. C. Truong, D. K. Mishra, *Environ. Chem. Lett.* **2020,** DOI: 10.1007/s10311-020-01121-7; c) Y. Yang, J.-W. Lee, *Chem. Sci.* **2019**, *10*, 3905-3926.

[2] a) A. Rehman, F. Saleem, F. Javed, A. Ikhlaq, S. W. Ahmad, A. Harvey, *J. Environ. Chem. Eng.* **2021**, *9*, 105113; b) L. Guo, K. J. Lamb, M. North, *Green Chem.* **2021**, *23*, 77-118.

[3] a) X.-F. Liu, M.-Y. Wang, L.-N. He, *Curr. Org. Chem.* **2017**, *21*, 698-707; b) S. Pulla, C. M. Felton, P. Ramidi, Y. Gartia, N. Ali, U. B. Nasini, A. Ghosh, *J. CO2 Util.* **2013**, *2*, 49-57.

[4] A. Modak, P. Bhanja, S. Dutta, B. Chowdhury, A. Bhaumik, *Green Chem.* **2020**, *22*, 4002-4033.

[5] a) S. G. Davies, A. M. Fletcher, P. M. Roberts, J. E. Thomson, *Org. Biomol. Chem.* **2019**, *17*, 1322-1335; b) A. Nazari, M. M. Heravi, V. Zadsirjan, *J. Organomet. Chem.* **2021**, *932*, 121629; c) M. M. Heravi, V. Zadsirjan, B. Farajpour, *RSC Adv.* **2016**, *6*, 30498-30551.

[6] a) M. Yan, L. Xu, Y. Wang, J. Wan, T. Liu, W. Liu, Y. Wan, B. Zhang, R. Wang, Q. Li, *Drug Dev. Res.* **2020**, *81*, 402-418; b) C. Roger, J. A. Roberts, L. Muller, *Clin. Pharmacokinet.* **2018**, *57*, 559-575.

[7] a) T. Niemi, T. Repo, *Eur. J. Org. Chem.* **2019**, 1180-1188; b) M. R. Barbachyn, in *Antibacterials: Volume II* (Eds.: J. F. Fisher, S. Mobashery, M. J. Miller), Springer International Publishing, Cham, **2018**, pp. 97-121; c) P. S. Jadhavar, M. D. Vaja, T. M. Dhameliya, A. K. Chakraborti, *Curr. Med. Chem.* **2015**, *22*, 4379-4397; d) M. Nasibullah, F. Hassan, N. Ahmad, A. R. Khan, and M. Rahman, *Adv. Sci. Eng. Med.* **2015**, *7*, 91-111.

[8] A. Zahedi Bialvaei, M. Rahbar, M. Yousefi, M. Asgharzadeh, H. Samadi Kafil, *J. Antimicrob. Chemother.* **2017**, *72*, 354-364.

[9] a) D. McBride, T. Krekel, K. Hsueh, M. J. Durkin, *Expert Opin. Drug Metab. Toxicol.* **2017**, *13*, 331-337; b) A. A. Carena, M. E. Stryjewski, *Expert Rev. of Clin. Pharmacol.* **2020**, *13*, 577-592; c) S. D. Burdette, R. Trotman, *Clin. Infect. Dis.* **2015**, *61*, 1315-1321.

[10] F. Moureau, J. Wouters, D. P. Vercauteren, S. Collin, G. Evrard, F. Durant, F. Ducrey, J. J. Koenig, F. X. Jarreau, *Eur. J. Med. Chem.* **1992**, *27*, 939-948.

[11] J. Furtado Campos, M. C. Pereira, W. L. B. de Sena, C. G. de Barros Martins, J. Ferreira de Oliveira, C. A. da Cruz Amorim, M. J. Barreto de Melo Rêgo, M. G. da Rocha Pitta, M. do Carmo Alves de Lima, M. G. da Rocha Pitta, I. da Rocha Pitta, *Pharmacol. Rep.* **2017**, *69*, 633-641.

[12] C. Phung, A. R. Pinhas, *Tetrahedron Lett.* **2010**, *51*, 4552-4554.

[13] S. Arshadi, A. Banaei, S. Ebrahimiasl, A. Monfared, E. Vessally, *RSC Adv.* **2019**, *9*, 19465-19482.

[14] C. Phung, D. J. Tantillo, J. E. Hein, A. R. Pinhas, *J. Phys. Org. Chem.* **2018**, *31*, e3735.

[15] a) B. Xu, P. Wang, M. Lv, D. Yuan, Y. Yao, *ChemCatChem* **2016**, *8*, 2466-2471; b) D. Adhikari, A. W. Miller, M.-H. Baik, S. T. Nguyen, *Chem. Sci.* **2015**, *6*, 1293-1300.

[16] a) H. Xu, X.-F. Liu, C.-S. Cao, B. Zhao, P. Cheng, L.-N. He, *Adv. Sci.* **2016**, *3*, 1600048; b) A. A. L. Goncalves, A. C. Fonseca, J. F. J. Coelho, A. C. Serra, *Curr. Green Chem.* **2015**, *2*, 43-65; c) T.-d. Hu, Y.-h. Ding, *Organometallics* **2020**, *39*, 505-515; d) X.-M. Kang, L.-H. Yao, Z.-H. Jiao, B. Zhao, *Chem. Asian J.* **2019**, *14*, 3668-3674. c) Y. Du, Y. Wu, A.-H. Liu, L.-N. He, *J. Org. Chem.* **2008**, *7*3, 4709–4712.

[17] a) D. Intrieri, C. Damiano, P. Sonzini, E. Gallo, *J. Porphyr. Phthalocyanines* **2019**, *23*, 305-328; b) V. Saptal, D. B. Shinde, R. Banerjee, B. M. Bhanage, *Catal. Sci. Technol.* **2016**, *6*, 6152-6158; c) X. Wang, W.-Y. Gao, Z. Niu, L. Wojtas, J. A. Perman, Y.-S. Chen, Z. Li, B. Aguila, S. Ma, *Chem. Commun.* **2018**, *54*, 1170-1173; d) Y. Chen, R. Luo, Z. Yang, X. Zhou, H. Ji, *Sustain. Energy Fuels* **2018**, *2*, 125-132.

[18] a) D. Carminati, E. Gallo, C. Damiano, A. Caselli, D. Intrieri, *Eur. J. Inorg. Chem.* **2018**, *2018*, 5258-5262; b) C. Damiano, P. Sonzini, D. Intrieri, E. Gallo, *J. Porphyr. Phthalocyanines* **2020**, *24*, 809-816.

[19] P. Sonzini, C. Damiano, D. Intrieri, G. Manca, E. Gallo, *Adv. Synth. Catal.* **2020**, *362*, 2961-2969.

[20] a) D. Intrieri, S. Le Gac, A. Caselli, E. Rose, B. Boitrel, E. Gallo, *Chem. Commun.* **2014**, *50*, 1811-1813; b) D. M. Carminati, D. Intrieri, A. Caselli, S. Le Gac, B. Boitrel, L.Toma, L. Legnani, E. Gallo *Chem. Eur.J.* **2016**, *22*, 13599–13612.

[21] a) C. Maeda, S. Sasaki, T. Ema, *ChemCatChem* **2017**, *9*, 946-949; b) Y. Lu, Z. Chang, S. Zhang, S. Wang, Q. Chen, L. Feng, Z. Sui, *J. Mater. Sci.* **2020**, *55*, 11856-11869; c) C. Maeda, T. Taniguchi, K. Ogawa, T. Ema, *Angew. Chem. Int. Ed.* **2015**, *54*, 134-138.

[22] D. Intrieri, C. Damiano, S. Rizzato, R. Paolesse, M. Venanzi, D. Monti, M. Savioli, M. Stefanelli, E. Gallo, *New J. Chem.* **2018**, *42*, 15778-15783.

[23] J. S. Lindsey, K. A. MacCrum, J. S. Tyhonas, Y.-Y. Chuang, *J. Org. Chem.* **1994**, *59*, 579-587.

[24] B. L. Auras, S. De Lucca Meller, M. P. da Silva, A. Neves, L. H. Z. Cocca, L. De Boni, C. H. da Silveira, B. A. Iglesias, *Appl. Organomet. Chem.* **2018**, *32*, e4318.

[25] J. S. Lindsey, R. W. Wagner, *J. Org. Chem.* **1989**, *54*, 828-836.

[26] J. L. Sessler, A. Mozaffari, M. R. Johnson, in *Org. Synth., Vol. 70*, **1991**, pp. 68-77.

[27] S. S. Eaton, G. R. Eaton, *J. Am. Chem. Soc.* **1975**, *97*, 3660-3666.

[28] C.-W. Zhuo, Y.-S. Qin, X.-H. Wang, F.-S. Wang, *Chin. J. Polym. Sci.* **2018**, *36*, 252-260.

[29] A. D. Adler, F. R. Longo, W. Shergalis, *J. Am. Chem. Soc.* **1964**, *86*, 3145-3149.

[30] S. Fantauzzi, E. Gallo, A. Caselli, C. Piangiolino, F. Ragaini, S. Cenini, *Eur. J. Org. Chem.* **2007**, 6053-6059.

[31] S. Grimme, *J. Chem. Phys.* **2006**, *124*, 034108

[32] Gaussian 16, Revision C.01, M. J. Frisch, G. W. Trucks, H. B. Schlegel, G. E. Scuseria, M. A. Robb, J. R. Cheeseman, G. Scalmani, V. Barone, G. A. Petersson, H. Nakatsuji, X. Li, M. Caricato, A. V. Marenich, J. Bloino, B. G. Janesko, R. Gomperts, B. Mennucci, H. P. Hratchian, J. V. Ortiz, A. F. Izmaylov, J. L. Sonnenberg, D. Williams-Young, F. Ding, F. Lipparini, F. Egidi, J. Goings, B. Peng, A. Petrone, T. Henderson, D. Ranasinghe, V. G. Zakrzewski, J. Gao, N. Rega, G. Zheng, W. Liang, M. Hada, M. Ehara, K. Toyota, R. Fukuda, J. Hasegawa, M. Ishida, T. Nakajima, Y. Honda, O. Kitao, H. Nakai, T. Vreven, K. Throssell, J. A. Montgomery, Jr., J. E. Peralta, F. Ogliaro, M. J. Bearpark, J. J. Heyd, E. N. Brothers, K. N. Kudin, V. N. Staroverov, T. A. Keith, R. Kobayashi, J. Normand, K. Raghavachari, A. P. Rendell, J. C. Burant, S. S. Iyengar, J. Tomasi, M. Cossi, J. M. Millam, M. Klene, C. Adamo, R. Cammi, J.

W. Ochterski, R. L. Martin, K. Morokuma, O. Farkas, J. B. Foresman, and D. J. Fox, Gaussian, Inc., Wallingford CT, 2016.

[33] a) V. Barone, M. Cossi, *J. Phys. Chem. A* **1998**, *102*, 1995-2001; b) M. Cossi, N. Rega, G. Scalmani, V. Barone, *J. Comput. Chem.* **2003**, *24*, 669-681.

Entry for the Table of Contents

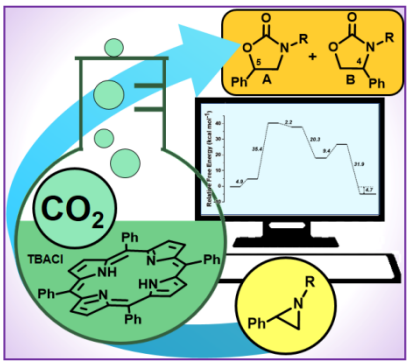

The cycloaddition of CO_2 to *N*-alkyl aziridines was efficiently promoted by a low-loading of free-porphyrin/TBACl combination and the presence of a metallic promoter was not required. The reaction scope was studied and DFT calculations suggested a mechanism of the *N*-alkyl oxazolid-2-one formation.